$\eta(1-8) = 0.010$, giving $\Delta\chi = -2.80 \times 10^{-28}$ emu and $\delta\chi = 0.08 \times 10^{-28}$ emu; for D(10), using qcc(10) = 199.5 kHz and the experimental splitting, one finds $\eta(10) = 0.43$, which is larger than the theoretically estimated value of 0.28.

The calculated $\Delta\chi$ and $\delta\chi$ are equal to the ones in anthracene within a few percent. A $\Delta\chi$ value, reduced by 14%, would require $\eta(1-8) = 0.23$ and $\eta(10) = 0.60$ if the above qcc values are used; these values seem too extreme to be correct.

Two points should be stressed which both support the reliability of these calculations: first, in the analogous study of the fluorenyl carbanion,[4] the charge density differences between molecule and ion are comparable, but no alteration of the asymmetry parameter of the outer ring deuterons was necessary to account for the expected change in $\Delta\chi$; second, the line widths of D(1–8) in molecule and ion are about the same, as is expected if the qcc's, η's, and rotational correlation times are not changed noticeably. (In the same temperature range the viscosities of ether and HF are the same within a few percent.[9]) The larger qcc of D(10)

relative to that of D(1–8) is also reflected in its larger line width.

In the foregoing we have neglected the counterion BF_4^-, which in principle could affect the quadrupolar coupling in the deuterons of the cation; however, HF is strongly polar and ion-pair formation will be negligible.

So, the final conclusion is that going from the molecule to the ion, $\Delta\chi$ maximally changes by 4–5%, i.e., much less than expected.

(9) Simons, J. H.; Dresdner, R. D. *J. Am. Chem. Soc.* **1944,** *66,* 1070–1072.

Magnetic Properties of Manganese in the Photosynthetic O₂-Evolving Complex

Julio C. de Paula and Gary W. Brudvig*

Contribution from the Department of Chemistry, Yale University, New Haven, Connecticut 06511. Received October 9, 1984

Abstract: We report the continuous power saturation and temperature dependence of three EPR signals which are generated by low-temperature illumination of dark-adapted Photosystem II (PSII) membranes and are associated with the S_2 state of the O₂-evolving complex of photosynthesis. PSII membranes which are dark-adapted for 4 h at 0 °C and illuminated at 200 K for 2 min exhibit a S_2 state EPR signal which saturates easily ($P_{1/2} = 3.7$ mW at 6.0 K) and has an intensity maximum at 6.9 K under nonsaturating conditions. The S_2 state EPR signal obtained from 6-min dark-incubated samples illuminated at 160 K exhibits no intensity maximum in the 4.0–16.0 K range under nonsaturating conditions and saturates at higher microwave powers ($P_{1/2} = 37.1$ mW at 6.0 K). Finally, a third signal produced by 170 K illumination of 6-min dark-adapted membranes shows an intensity maximum at 5.9 K under nonsaturating conditions and is not saturated with our current experimental setup ($P_{1/2} > 156$ mW at 6.0 K). We conclude that each EPR spectrum originates from a thermally excited state of one of three distinct configurations of the manganese complex which is believed to make up the active site. The temperature dependence data are fitted to a model in which two paramagnetic sites are ferromagnetically exchange coupled. All three sets of data can be accounted for by varying the magnitude of the superexchange coupling constant.

It is currently accepted that the four-electron photooxidation of H_2O to O_2 catalyzed by the O₂-evolving center (OEC) of Photosystem II (PSII) occurs stepwise with the generation of five intermediate oxidation states known as S_i ($i = 0$ to 4) states.[1] Both the S_0 and S_1 states are stable in short-term dark-incubated chloroplasts or PSII membranes, where they are present in a 1:3 proportion, due to rapid back-reaction from the S_2 and S_3 states to the S_1 state.[2] The S_4 state is relatively unstable and quickly releases O_2, cycling the system back to the S_0 state.[1,2]

Since this S state scheme was first proposed, many attempts have been made to probe these photoactive intermediates spectroscopically.[3] Electron paramagnetic resonance (EPR) has been a helpful tool in the elucidation of this problem. Dismukes and Siderer[4] showed that irradiation of spinach chloroplasts with one

saturating laser flash quickly followed by freezing at 77 K produced a multiline EPR signal centered at $g = 2.0$. Later, Brudvig et al.[5] showed that an identical EPR signal could be obtained by continuously illuminating dark-adapted chloroplasts at 200 K, and then trapping at 77 K. The properties derived from this multiline EPR signal[5] agreed well with the properties of the S_2 state measured by thermoluminescence,[6] fluorescence,[7] and O_2 evolution[8] studies.

Efforts to account for the molecular species giving rise to the multiline EPR signal have pointed toward a manganese complex as a likely model. The involvement of manganese in O_2 evolution is well-known,[3] and computer simulations using antiferromagnetically exchange coupled mixed-valence manganese dimers as

(1) Kok, B.; Forbush, B.; McGloin, M. *Photochem. Photobiol.* **1970,** *11,* 457.

(2) Forbush, B.; Kok, B.; McGloin, M. *Photochem. Photobiol.* **1971,** *15,* 307.

(3) Amez, J. *Biochim. Biophys. Acta* **1983,** *726,* 1.

(4) Dismukes, G. C.; Siderer, Y. *Proc. Natl. Acad. Sci. U.S.A.* **1981,** *78,* 274.

(5) (a) Brudvig, G.; Casey, J.; Sauer, K. *Biochim. Biophys. Acta* **1983,** *723,* 361. (b) Brudvig, G.; Casey, J.; Sauer, K. In "The Oxygen Evolving System of Photosynthesis"; Inoue, Y., et al., Eds.: Academic Press: Tokyo, 1983; p 159.

(6) Inoue, Y.; Shibata, K. *FEBS Lett.* **1978,** *85,* 193.

(7) Butler, W. L.; Visser, J. W. M.; Simons, H. L. *Biochim. Biophys. Acta* **1973,** *292,* 140.

(8) Joliot, P.; Joliot, A.; Bouges, B.; Barbieri, G. *Photochem. Photobiol.* **1971,** *14,* 287.

models have been somewhat successful in duplicating the main spectral features of the S_2 state EPR signal.[4,9]

Recent work in this laboratory[10] has shown that three distinct EPR signals from the S_2 state can be observed. PSII membranes which were incubated in the dark for 4 h at 0 °C showed a light-induced multiline EPR signal with an optimum temperature for its generation at 200 K. In addition, illumination of short-term dark-adapted (6 min at 0 °C) membranes at 160 and 170 K produced two different EPR signals which were distinguished by the relative spread of their main hyperfine lines.

This paper presents the magnetic properties of the three EPR signals discussed above as probed by their continuous-wave power saturation and temperature dependence. By virtue of the non-Curie temperature dependence exhibited by these signals, we propose a model in which the EPR transitions originate from a thermally excited state of a ferromagnetically exchange coupled spin system. The differences in the temperature profile of the signals can be explained by this model if the magnitude of the superexchange coupling constant is allowed to vary.

Experimental Section

PSII membranes were prepared in darkness from 2-h dark-adapted market spinach according to Berthold et al.[11] except that all buffers contained 5 mM ethylenediaminetetraacetic acid (EDTA) and 1 g/L of bovine serum albumin (Sigma, Fraction V powder). Samples were stored at 77 K until use in the storage buffer which contained 20 mM 2·(N-morpholino)ethanesulfonic acid (MES)/NaOH, pH 6.0, 15 mM sodium chloride, 5 mM magnesium chloride, and 30% v/v ethylene glycol. The preparations used in this study exhibited rates of O_2 evolution which varied from 300 to 500 μmol of O_2/mg of Chl/h when assayed in the storage buffer with 250 μM dichlorobenzoquinone as an electron acceptor.

Pellets of PSII membranes were suspended in storage buffer to a chlorophyll concentration of approximately 6.0 mg/mL, according to the assay method of Arnon.[12] The resulting suspensions were held in 4 mm o.d. quartz EPR tubes.

Prior to dark adaptation in an ice/water slush, the samples were illuminated with a 60 W incandescent bulb (100 W/m²) for 2 min to allow for multiple turnovers of the OEC. Immediately after the predetermined period of dark incubation the samples were frozen in liquid nitrogen.

The S_2 state EPR signal was generated by the method of Brudvig et al.[5] EPR tubes containing dark-adapted PSII membranes were placed in a nitrogen flow apparatus cooled by an ethanol slush. After 3 min of thermal equilibration at the desired temperature (160–200 K), the samples were illuminated for 2 min with a 100 W quartz–halogen lamp (700 W/m²). The sample temperature was checked by using a carbon–glass resistor (Lake Shore Cryotronics) inserted in an EPR tube containing ethylene glycol.

EPR measurements were performed in a JEOL ME-3X X-band spectrometer interfaced to a DEC MINC-23 computer and equipped with an Oxford ESR-900 liquid helium cryostat. The temperature was checked with the carbon–glass resistor at the sample position. The temperature gradient over the sample was estimated by moving the carbon-glass resistor over the length of the resonant cavity. It was found that at the lowest flow rate of liquid helium used in this work (approximately 0.3 L/h) this gradient was of the order of 0.2 to 0.4 K and, thus, the maximum error in the temperature measurement was 0.4 K. The microwave power incident on the cavity was determined by using a General Microwave Model 476 power meter equipped with a General Microwave Model 4240C power head and was calibrated by using a nonsaturating standard Cr^{+3}/MgO sample.[13] Triplicate runs were performed for each power saturation curve presented in this paper, and the variation in the $P_{1/2}$ values was from 5 to 15%.

Results

Active and Resting States of the OEC. We previously found[10] that the PSII-OEC can exist in two states: a resting state present in long-term dark-adapted PSII membranes which produces an
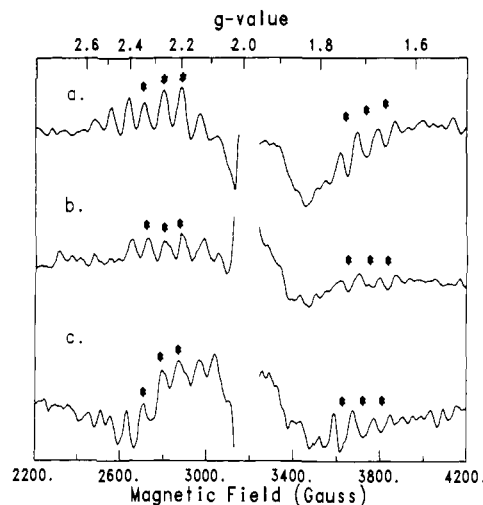
(9) Hansson, Ö.; Andréasson, L.-E. *Biochim. Biophys. Acta* **1982**, *679*, 261.

(10) Beck, W. F.; de Paula, J. C.; Brudvig, G. W. *Biochemistry*, in press.

(11) Berthold, D. A.; Babcock, G. T.; Yocum, C. F. *FEBS Lett.* **1981**, *134*, 231.

(12) Arnon, D. *Plant. Physiol.* **1949**, *24*, 1.

(13) Poole, C. P., Jr. "Electron Spin Resonance"; John Wiley and Sons: New York, 1983; p 597.

Figure 1. Dependence of the hyperfine structure of the S_2 state EPR spectra of PSII membranes on temperature of illumination: (a) 200 K illuminated, 4-h dark-adapted; (b) 160 K illuminated, 6-min dark-adapted; (c) 170 K illuminated, 6-min dark-adapted. Spectra shown are the difference between the spectrum after and before illumination: The $g = 2.0$ region is not shown. Instrumental conditions: microwave frequency, 8.81 GHz; microwave power, 10 mW; modulation frequency, 100 KHz; modulation amplitude, 20 G; sample temperature, 10 K. Relative scale factors on each spectrum were adjusted so that all three signals would be equally intense. The asterisks denote the peak positions used for data analysis.

S_2 state EPR signal (Figure 1a) with hyperfine structure and properties similar to those reported in the literature[5] and an active state present in short-term dark-adapted PSII membranes which gives rise to two different EPR signals upon low-temperature illumination. Active state membranes which were illuminated at 160 K generated an S_2 state signal (Figure 1b) with hyperfine features similar to the resting state spectrum obtained by 200 K illumination, except that in the latter, more intense low-field lines were apparent. When active state membranes were illuminated at 170 K or higher temperatures the resulting S_2 state spectrum (Figure 1c) showed a more complex hyperfine pattern than the 160 K generated spectrum, thus suggesting a change in the environment of the active site.

Continuous-Wave Power-Saturation Studies. The intensity, I, of an EPR line as a function of power is given by Rupp et al.[14] as

$$I = K[P^{0.5}/(1 + P/P_{1/2})^{0.5b}] \qquad (1)$$

where K is a constant proportional to the total number of spins; P is the microwave power in mW; $P_{1/2}$ is the power for half-saturation in mW, which is proportional to the product of the spin–lattice relaxation rate, T_1^{-1}, and the spin–spin relaxation rate, T_2^{-1}; and b is the inhomogeneity parameter which varies from 1 to 4 with increasing homogeneity in the first-derivative resonance line.

A convenient way to present power-saturation data is to plot log $(I/P^{1/2})$ vs. log P. In the nonsaturating limit, i.e., where $P \ll P_{1/2}$, this plot yields a straight line parallel to the abscissa, but as saturation occurs the plot begins to curve downward and becomes a straight line of slope $-0.5b$. The power at half-saturation can be determined graphically by extrapolating the straight-line parts of the plot and finding the value of the abscissa at the point of intersection. In this work the graphical method was chosen over a nonlinear least-squares fit to the data. If the line width remains constant over a temperature range, then b should also remain unchanged. Such is the case in all of our measurements. Therefore, we have chosen a fixed value for the slope of the saturated portion of the log $(I/P^{1/2})$ vs. log P plots throughout

(14) Rupp, H.; Rao, K. K.; Hall, D.; Cammack, R. *Biochim. Biophys. Acta* **1978**, *537*, 255.
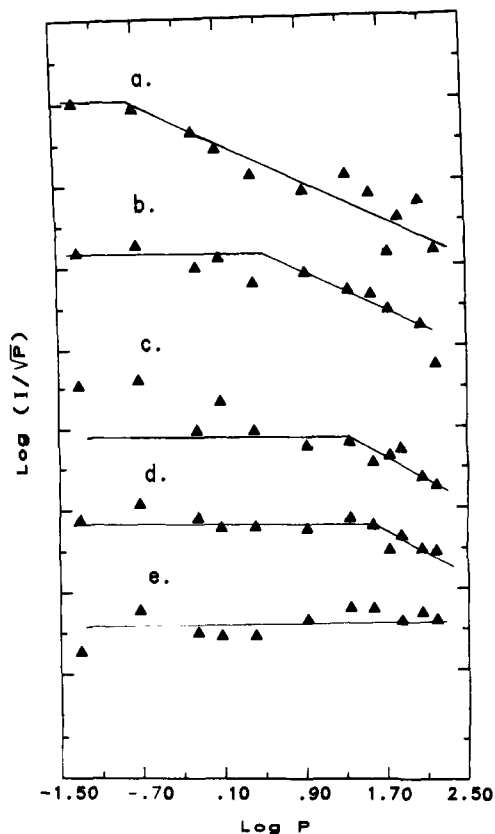
Figure 2. Power saturation at several temperatures of the EPR signal generated by illumination of 4-h dark-adapted PSII membranes at 200 K: (a) 4.5 K; (b) 6.0 K; (c) 6.8 K; (d) 8.0 K; (e) 10.0 K. Microwave power is given in mW. Signal intensities were determined as the peak-to-peak heights of the lines denoted by asterisks in Figure 1. The intersection of the straight lines through the data determines the value of $P_{1/2}$, as explained in the text. Each plot was arbitrarily offset along the y axis. The inhomogeneity parameter b was set to 1.4. Spectrometer conditions were the same as in Figure 1.

Figure 3. Power saturation at several temperatures of the EPR signal generated by illumination of 6-min dark-adapted PSII membranes at 160 K: (a) 5.8 K; (b) 6.0 K; (c) 7.0 K; (d) 8.5 K; (e) 9.0 K; (f) 10.0 K. Data analysis was the same as in Figure 2. Each plot was arbitrarily offset along the y axis. The inhomogeneity parameter b was set to 1.8. Spectrometer conditions were the same as in Figure 1.

the temperature range for each set of data.

Figures 2, 3, and 4 show the power saturation of the three S_2 state EPR signals between 4.5 and 10.0 K. The S_2 state EPR signal from the resting state illuminated at 200 K saturates most easily ($P_{1/2}$ = 3.7 mW at 6 K). In the active state, there is noticeable difference in power saturation between the signals obtained by 160 and 170 K illumination: $P_{1/2}$ = 37.1 mW and >156 mW at 6 K, respectively.

Spin-Relaxation Mechanisms. Our power saturation data are discussed below in terms of two relaxation mechanisms known as the Raman and Orbach processes (for a detailed discussion, see ref 15). In the Raman mechanism, a spin flip results from the excitation of a paramagnet to a virtual energy state by a lattice phonon followed by emission of a higher energy phonon. If a Raman process is responsible for the relaxation of a paramagnet, T_1^{-1} is expected to vary with temperature as T^n, where usually $3 < n < 9$. This mode of relaxation differs from an Orbach mechanism, where excitation to and emission from a real excited state of the spin system occurs. For an Orbach process, the relaxation rate is proportional in the high-temperature limit to $\exp(-\Delta/kT)$, where Δ is the energy separation between the excited and ground states.

Figure 5 shows fits to Raman and Orbach mechanisms of the temperature variation of $P_{1/2}$ over the range 4.5–8.0 K for the resting S_2 state signal generated by 200 K illumination and the active S_2 state signal generated by 160 K illumination. It is seen that the saturation data for these signals can be satisfactorily described by a Raman mechanism with a $T^{2.7}$ dependence in the active state (Figure 5a) and a $T^{9.5}$ dependence in the resting state (Figure 5b). The data can be fitted equally well, however, by an Orbach mechanism with an excited state lying 13.7 cm⁻¹ above
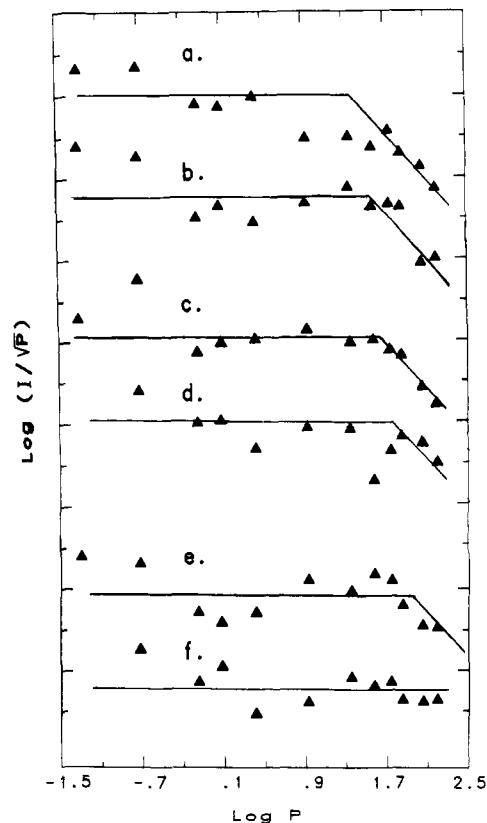
the relaxing spin system in the active state (Figure 5c) or 41.6 cm⁻¹ in the resting state (Figure 5d). The ambiguity in our assignment of the relaxation mechanism comes partly from the limited temperature range over which we could observe saturation of the EPR signals in this study. Our data do allow us, however, to point out a few possible explanations for the differences in power saturation of the S_2 state signals in the active state (160 K illumination) and in the resting state. The fit to a Raman mechanism requires variation in exponents from 2.7 in the active state illuminated at 160 K to 9.5 in the resting state illuminated at 200 K. Such a drastic change may not be realistic. On the other hand, it is easier to rationalize the power saturation of the three S_2 state EPR signals in terms of an Orbach mechanism. The faster relaxation rate in the active state could be explained by a smaller energy gap between the EPR observable state and an excited spin state. Alternatively, a neighboring spin may be providing an additional relaxation pathway for the S_2 state spin system. If a neighboring spin influences the relaxation of the S_2 state EPR signal species, then as the OEC changes from the active to the resting state, the interacting spin must also undergo a configurational change, such as a high to low spin conversion or a change in distance, which makes it a poorer relaxer.

Hansson et al.[16] have reported power saturation data between 3.7 and 6.3 K on a multiline signal which is generated by continuously illuminating chloroplasts while freezing to 77 K. They were able to fit their data to an Orbach mechanism with an excited state 29 cm⁻¹ above the ground state. However, due to the different method employed by Hansson et al.[16] to generate the S_2

(15) (a) Abragam, A.; Bleaney, B. "Electron Paramagnetic Resonance of Transition Metal Ions"; Oxford: London, 1970. (b) Allen, J. P.; Colvin, J. T.; Stinson, D. G.; Flynn, C. P.; Stapleton, H. J. *Biophys. J.* **1982**, *38*, 299.

(16) Hansson, Ö.; Andréasson, L.-E.; Vänngård, T. In "Advances in Photosynthesis Research", Sybesma, C., Ed.: Nijhoff/Junk Publishers: The Hague, 1984; Vol. 1, p 307.
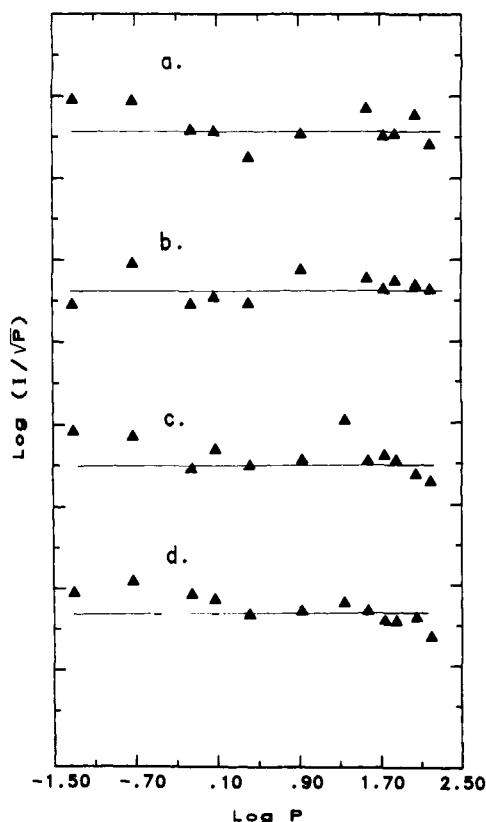
Figure 4. Power saturation at several temperatures of the EPR signal generated by illumination of 6-min dark-adapted PSII membranes at 170 K: (a) 6.0 K; (b) 7.0 K; (c) 8.0 K; (d) 10.0 K. Data analysis was the same as in Figure 2. Each plot was arbitrarily offset along the y axis. Spectrometer conditions were the same as in Figure 1.
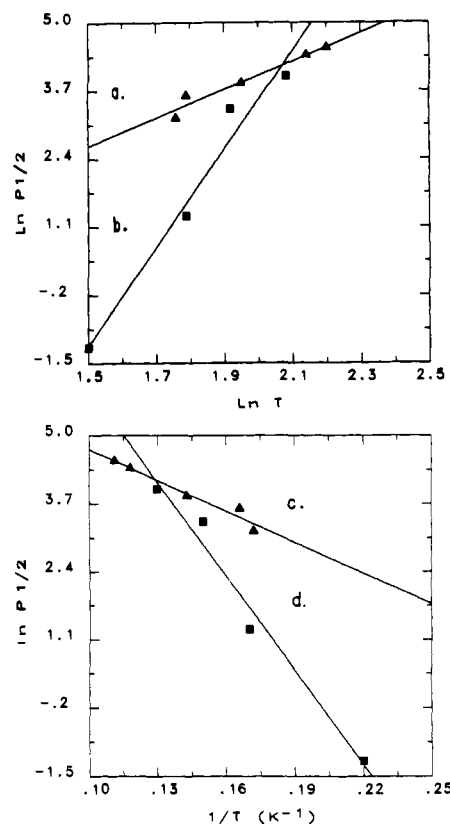

Figure 5. Dependence on temperature of $P_{1/2}$ values extracted graphically from Figures 2 and 3. Slopes were calculated by linear regression of the data. Powers are given in mW and temperature in K. (a) Active state PSII illuminated at 160 K, slope = 2.7; (b) resting state PSII illuminated at 200 K, slope = 9.5; (c) active state PSII illuminated at 160 K, slope = −19.7 K; (d) resting state PSII illuminated at 200 K, slope = $-\Delta/k$ = −59.8 K.

state EPR signal a direct comparison to our data may not be in order.

Temperature Dependence Studies. EPR transitions originating from a ground-state Kramer's doublet ($s = {}^1/_2$) with no low-lying thermally accessible excited states should follow a Curie law behavior, i.e., the signal amplitude should increase with decreasing temperature as the $m_s = {}^1/_2$ state becomes more populated. If a thermally populated excited state gives rise to the signal, however, a deviation from the Curie law will occur as kT approaches a value at which depopulation to a lower energy level occurs. At this point, as the temperature is lowered further, the signal intensity decreases. Care must be exercised to ensure that an apparent intensity maximum does not result from power saturation at lower temperatures.[15]

Figure 6a shows that the resting state multiline EPR signal exhibited a non-Curie temperature behavior with an intensity maximum at 6.9 K. The data in Figure 2 clearly show that the phenomenon is not caused by a power-saturation effect. In active state membranes illuminated at 160 K, the amplitude of the light-induced signal shows apparent Curie law dependence over the temperature range 4.0–16.0 K (Figure 6b). The active state signal produced by 170 K illumination has non-Curie dependence (Figure 6c, saturation data on Figure 4) with an intensity maximum at 5.9 K.

Hansson et al.[16] have also studied the temperature dependence of the multiline EPR spectrum generated by continuously illuminating samples while slowly freezing to 77 K. They observe Curie behavior in the range 3.7–6.3 K. Due to their method of sample illumination, it is very likely that their S_2 state signals originate from the active state of the OEC. This may account for the similarities in temperature dependence between their S_2 state signals and our 160 K generated spectrum.

Discussion

The continuous power-saturation and temperature dependence results presented here provide further support for our conclusion

that the three EPR signals from the S_2 state first reported by Beck et al.[10] originate from three different configurations of the Mn active site of the PSII-OEC. Below 7.5 K, the resting state multiline signal saturates more easily than the active state signal generated by 160 K illumination. On the other hand, the saturation of the EPR signal generated by illumination at 170 K of active state membranes cannot be observed under the present experimental conditions ($P_{1/2} > 156$ mW). Therefore, it is clear that the relaxation properties of the spin system are greatly affected by changes in length of dark adaptation and illumination temperature.

The multitude of hyperfine lines in the S_2 state spectrum is a strong indication that a multinuclear Mn complex is involved. As mentioned previously, computer simulations of the S_2 state EPR signal have been attempted. Reasonable success has been attained with antiferromagnetically exchange coupled Mn(III)–Mn(IV) and Mn(II)–Mn(III) pairs as models for the site.[4,9] However, the calculated spectra failed to reproduce the positions of most of the high-field lines, as well as the overall intensity pattern. Furthermore, a clear distinction between antiferromagnetic and ferromagnetic exchange coupling cannot be achieved solely by simulating the signal; provided that the interaction is sufficiently strong, the simulated spectra will appear identical regardless of which exchange mechanism is invoked. The temperature dependence of the signals, however, can discriminate between ferromagnetic and antiferromagnetic exchange interactions.

Our temperature dependence data show that an excited-state spin manifold is the origin of at least two of the S_2 state EPR signals. In choosing a model to rationalize the data, we have assumed that they originate from a thermally excited $s = {}^1/_2$ spin level of a ferromagnetically exchange coupled system. Evidence supporting the statement that the S_2 state EPR signal arises from an $s = {}^1/_2$ state comes from orientation studies. Hansson et al.[16] have detected no anisotropy in their signals which were generated
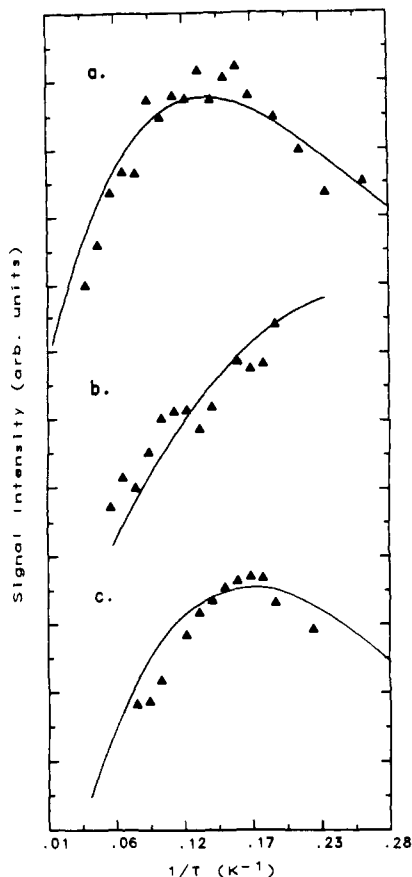
Figure 6. Temperature dependence of the intensity of the multiline EPR signals at 0.05 mW. The lines through the data are computer fits to eq 3 from the text with the energy levels obtained from the diagonalization of H_{dimer}. $D_2 = 3.0$ cm^{-1} for all three fits. (a) Resting state illuminated at 200 K, $J = -3.5$ cm^{-1}; (b) active state illuminated at 160 K, $J = -0.8$ cm^{-1}; (c) active state illuminated at 170 K, $J = -2.5$ cm^{-1}. Data analysis was the same as in Figure 2. Spectrometer conditions were the same as in Figure 1.

by illumination while freezing to 77 K. More recently, Rutherford[17] has observed no large-scale anisotropy in the EPR signal produced by 200 K illumination of PSII membranes. This is the behavior expected from a transition within an $s = {}^1/_2$ state with small anisotropy in the g values and hyperfine couplings.[15] A nearly isotropic EPR spectrum will not be observed from an $s > {}^1/_2$ state unless the paramagnetic site has a high degree of symmetry, an unlikely situation in the present case.

Inspection of Figure 6 shows that the experimental temperature curves exhibit rather sharp peaks. Therefore, only a small number of states lie below the spectroscopically observed state. Computer fits to the data (see below) show that the number of states below the EPR observable state is on the order of four.

The simplest model which can accommodate all the above restrictions is that which consists of ferromagnetically exchange coupled $s_1 = {}^1/_2$ and $s_2 = 1$ spins, where $s = |s_1 - s_2| = {}^1/_2$ or $s = |s_1 + s_2| = {}^3/_2$.

The intensity of an EPR transition, $I(T)$, arising from an $s = {}^1/_2$ Kramer's doublet varies with temperature according to

$$I(T) =$$
$$K[\exp(h\nu/2kT) - \exp(-h\nu/2kT)]/[\sum_i N_i \exp(-W_i/kT)] \quad (2)$$

where K is a proportionality constant, and W_i is the energy of the spin level with degeneracy N_i. The numerator reflects the population difference between the $m_s = {}^1/_2$ and the $m_s = -{}^1/_2$ levels in the $s = {}^1/_2$ state. In the limit $kT \gg h\nu$ or $T \gg 0.4$ K at X-band, we finally have

(17) Rutherford, A. W. *Biochim. Biophys. Acta*, submitted.

$$I(T) = (K'/T)[1/\sum_i N_i \exp(-W_i/kT)] \quad (3)$$

The most important contributions to the energy W_i are expected to come from exchange and spin–spin coupling effects. Thus, the Hamiltonian for two interacting spins can be written as

$$\hat{H}_{dimer} = \hat{H}_{ex} + \hat{H}_{ss} \quad (4)$$

where, assuming an isotropic superexchange coupling

$$\hat{H}_{ex} = J\hat{s}_1 \cdot \hat{s}_2 = J/2(\hat{s}^2 - \bar{s}_1{}^2 - \hat{s}_2{}^2) \quad (5)$$

where $\hat{s} = \bar{s}_1 + \hat{s}_2$ is the total spin operator. As we have written $\hat{H}_{ex}$, ferromagnetic exchange coupling occurs when $J < 0$. In this case the level $|s_1 - s_2|$ will be the highest excited state. The situation is reversed if $J > 0$, where antiferromagnetic exchange coupling occurs. The spin–spin interaction, $\hat{H}_{ss} = \hat{s}_1 \cdot D_1 \cdot \hat{s}_1 + \hat{s}_2 \cdot D_2 \cdot \hat{s}_2$, is given by

$$\hat{H}_{ss} = D_1[\hat{s}_{1z}{}^2 - {}^1/_3 s_1(s_1 + 1)] + D_2[\hat{s}_{2z}{}^2 - {}^1/_3 s_2(s_2 + 1)] \quad (6)$$

assuming $E = 0$.

The energy levels are obtained by diagonalizing $\hat{H}_{dimer}$ in the $|s, m_s\rangle$ representation. The non-zero matrix elements are given by

$$\langle {}^3/_2, {}^3/_2 | \hat{H}_{dimer} | {}^3/_2, {}^3/_2 \rangle = J/2 + D_2/3 \quad (7a)$$

$$\langle {}^3/_2, {}^1/_2 | \hat{H}_{dimer} | {}^3/_2, {}^1/_2 \rangle = J/2 - D_2/3 \quad (7b)$$

$$\langle {}^1/_2, {}^1/_2 | \hat{H}_{dimer} | {}^1/_2, {}^1/_2 \rangle = -J \quad (7c)$$

$$\langle {}^3/_2, +{}^1/_2 | \hat{H}_{dimer} | {}^1/_2, +{}^1/_2 \rangle = \quad (7d)$$

$$\langle {}^1/_2, +{}^1/_2 | \hat{H}_{dimer} | {}^3/_2, +{}^1/_2 \rangle = \frac{(2)^{1/2}}{3} D_2 \quad (7e)$$

$$\langle {}^3/_2, -{}^1/_2 | \hat{H}_{dimer} | {}^1/_2, -{}^1/_2 \rangle = \quad (7f)$$

$$\langle {}^1/_2, -{}^1/_2 | \hat{H}_{dimer} | {}^3/_2, -{}^1/_2 \rangle = -\frac{(2)^{1/2}}{3} D_2 \quad (7g)$$

The temperature dependence curves of the multiline EPR signals could be satisfactorily fitted with eq 3 (Figure 6) by using $D_2 = 3.0$ cm^{-1} and J values of -3.5 (resting state), -2.5 (170 K illuminated active state), and >-0.8 cm^{-1} (160 K illuminated active state).

As previously discussed, the S_2 state EPR signals all show hyperfine interactions diagnostic of manganese. Furthermore, four Mn are known to exist in the OEC.[3] How can the $s_1 = {}^1/_2$ and $s_2 = 1$ sites that arise from our fits to the temperature dependence data be accommodated by Mn (or other components) in the OEC?

The $s_1 = {}^1/_2$ spin could be the ground state of a Mn(II)–Mn(III) or Mn(III)–Mn(IV) dimer which is strongly antiferromagnetically exchange coupled, such that higher excited states would not contribute significantly to the coupling to the $s_2 = 1$ spin. The nature of the $s_2 = 1$ species is less clear. One possibility is low-spin Mn(III). Its complexes, however, are rare,[18] and apparently only in cyanide complexes is the ligand field strong enough to overcome the electron-pairing energy. The presence of low-spin Mn(III) in the S_2 state of the OEC cannot be completely ruled out, however, since the ligand environment around the active site may favor its existence. Alternatively, low-spin Fe(IV) could be the $s = 1$ ion which couples to the antiferromagnetic Mn dimer to give rise to the S_2 state EPR signals. An oxo form of low-spin Fe(IV) has been thought to be present in compound II of horseradish peroxidase.[19] Furthermore, Casey and Sauer[20] have suggested that an iron species acts as an electron carrier in the OEC and gives rise to a $g = 4.1$ EPR signal which

(18) Cotton, F. A.; Wilkinson, G. "Advanced Inorganic Chemistry"; John Wiley and Sons: New York, 1980; p 744.
(19) Morishima, I.; Ogawa, S. *Biochemistry* **1978**, *17*, 4384.
(20) Casey, J. L.; Sauer, K. *Biochim. Biophys. Acta* **1984**, *767*, 21.

can be trapped by continuous illumination at 140 K at the expense of generation of the S_2 state EPR signal. The moderately large zero-field splitting parameter D_2 required to fit our data (3.0 cm^{-1}) can be explained by a strong axially symmetric crystal field around the $s_2 = 1$ spin.[15]

If the $s_1 = \frac{1}{2}$ spin is indeed the ground state of an antiferromagnetic Mn dimer, then there must be excited states above the state giving rise to the EPR signals. As discussed earlier, the presence of an excited state provides a relaxation pathway for the spin system via an Orbach mechanism. Therefore, the values of Δ obtained from our power saturation data may reflect the extent of exchange coupling within the dimer. As an example, we considered a trimer consisting of $s_1 = 2$, $s_2 = \frac{3}{2}$, and $s_3 = 1$, which could arise from a site consisting of Mn(III) ($s_1 = 2$), Mn(IV) ($s_2 = \frac{3}{2}$), and low-spin Fe(IV) ($s_3 = 1$), where $J_{12} > 0$, $J_{13} < 0$, and $J_{23} < 0$. Provided that $|J_{12}| > |J_{23}|$ and $|J_{12}| > |J_{13}|$, the ground and lowest excited states of this trimer will have $s = \frac{3}{2}$ and $s = \frac{1}{2}$, respectively. The exchange Hamiltonian for three interacting spins can be written as $\hat{H}_{ex} = \sum_{i<k} J_{ik}\hat{s}_i\cdot\hat{s}_k$ and the spin–spin interaction is given by $\hat{H}_{ss} = \sum_i \hat{s}_i\cdot D_i\cdot\hat{s}_i$.

The energy levels were obtained by diagonalizing $\hat{H}_{trimer}$ in the uncoupled representation $|s_1s_2s_3m_1m_2m_3\rangle$, where

$$\hat{H}_{ex} = \sum_{i<k} J_{ik}[\frac{1}{2}(\hat{s}_{i+}\hat{s}_{k-} + \hat{s}_{i-}\hat{s}_{k+}) + \hat{s}_{iz}\hat{s}_{kz}] \tag{8}$$

and

$$\hat{H}_{ss} = \sum_i D_i[\hat{s}_{iz}^2 - \frac{1}{3}s_i(s_i + 1)] + \frac{1}{2}E_i(\hat{s}_{i+}^2 + \hat{s}_{i-}^2) \tag{9}$$

It was assumed that $E_i = 0.0$ cm^{-1} and that $J_{13} = J_{23} = J_2$ and $J_{12} = J_1$. In the case of the active S_2 state EPR signal generated by 170 K illumination, it was assumed that the value of Δ is the same as that for the active state obtained by 160 K illumination. The temperature-dependence data could be fitted by using J_2 values which were identical with the J values obtained from the previous model and $D_3 = 3.0$ cm^{-1}. The values of J_1 which fitted

the power-saturation data were 34.0 (resting state) and 12.7 cm^{-1} (active state).

Conclusions

The data presented in this paper show that the S_2 state EPR signals from the OEC arise from the interaction of more than one paramagnetic site. However, our temperature dependence data cannot be accounted for by a simple Mn dimer model, unless such a dimer arises from a ferromagnetic exchange coupling of low-spin forms of Mn. As noted above, low-spin Mn complexes are rare and not likely to be present in the OEC. A more reasonable model for the species giving rise to the S_2 state EPR signal is one in which an antiferromagnetically exchange coupled Mn(III)–Mn(IV) dimer is ferromagnetically exchange coupled to another site with $s = 1$. This second site could possibly be low-spin Mn(III), low-spin Fe(IV), or even a second Mn dimer.

We assign the S_2 state EPR signal to a thermally populated $s = \frac{1}{2}$ state. Therefore, if our interpretation of the data is correct, an EPR signal from the $s = \frac{3}{2}$ ground state should be observable at low temperature. This signal is expected to be anisotropic and, therefore, difficult to detect. Current efforts in this laboratory are directed at using the ferromagnetic exchange coupling scheme to accurately simulate the three S_2 state EPR spectra and attempting to observe EPR signals from the $s = \frac{3}{2}$ ground state of the S_2 state of the OEC.

A New Method for Obtaining Isotopic Fractionation Data at Multiple Sites in Rapidly Exchanging Systems

Ronald M. Jarret and Martin Saunders*

Contribution from the Sterling Chemistry Laboratory, Yale University, New Haven, Connecticut 06511. Received August 6, 1984

Abstract: A new method for rapidly and conveniently obtaining isotopic fractionation factors in dilute aqueous solutions of compounds containing rapidly exchanging OH, NH, and SH groups is described. Shifts in the positions of NMR peaks for spectroscopically observable nuclei induced by isotopic substitution are the basis of this procedure which has the unique capability of separately measuring the isotopic exchange constants simultaneously for several different groups in the same molecule. The results for a series of alcohols, amines, thiols, phenols, acids, and amides with use of ^{13}C NMR spectroscopy are reported. Atypically low values of K_{frac} are observed in several cases, indicating that there are strong internal hydrogen bonds in competition with those to water, yielding conformational information.

For an isotopic exchange reaction

$$HA + DB \underset{\phantom{K_{frac}}}{\overset{K_{frac}}{\rightleftharpoons}} DA + HB \tag{1}$$

the equilibrium constant K_{frac} is known as the fractionation factor. Many molecules containing OH, NH, and SH groups exchange hydrogen and deuterium rapidly with hydroxylic solvents, setting up such equilibria. These fractionation factors are closely related to details of molecular structure and are sensitive to changes in factors like hydrogen bonding. Strong internal hydrogen bonds

(in competition with those to the solvent) should be indicators of the conformation of flexible molecules.

Existing and established experimental methods cannot conveniently measure fractionation factors for hydrogen–deuterium exchange in dilute aqueous solution,[1] nor can previously reported techniques obtain information about individual exchangeable sites

(1) For a review of isotope effects see: (a) M. Wolfsberg, *Acc. Chem. Res.*, **5**, 225 (1972). (b) M. Wolfsberg, *Annu. Rev. Phys. Chem.*, **20**, 449 (1969).